Fluorescent core–shell magnetic nanoparticles by type II photoinitiated polymerisation

Maylis Garnier, Tugrul Cem Bicak, Michèle Sabbah, Nébéwia Griffete

COMMUNICATION

Fluorescent Core-Shell Magnetic Nanoparticles by Type II Photoinitiated Polymerisation

Maylis Garnier[a b], Tugrul Cem Bicak[a], Michèle Sabbah[b]* and Nébéwia Griffete[a]*

We report a fluorescent monomer-free method for the synthesis of fluorescent and stable magnetic nanocomposites by type II photoinitiated polymerisation, where benzophenone (BP) acts as a photosensitiser and rhodamine B (RhB) as hydrogen donor. The method allows the in-situ synthesis of fluorescent thin polymer shell layers around nanoparticles by UV irradiation.

Core-shell polymeric nanoparticles, which consist of an inorganic core coated with an organic polymer shell layer, are important class of hybrid nanomaterials and have found many applications in material science.[1,2,3] Conventionally, these nanocomposites are prepared by functionalisation of the inorganic core with a suitable vinyl monomer or an initiator, followed by polymerisation via grafting from or grafting-to processes. [4,5,6,7]

Introduction of fluorescent properties into magnetic nanoparticles (MNs) paves the way for a new class of functional materials, which have been proven to be useful in a wide range of applications including pollutant detection and recovery,[8] biomedical imaging[9,10,11] and drug delivery.[12,13] For the vast majority of these applications, fluorescence is either an essential part of detection or sensing, or it brings additional features facilitating the evaluation of those nanomaterials by making them easily detectable under fluorescence. Introduction of magnetic properties into nanoparticles not only allows easy recovery of the particles using a magnet, but also it brings additional properties such as magnetic hyperthermia and photothermia. To obtain MNs with fluorescent properties, several approaches have been developed until now, such as the post-functionalisation of core-shell particles using a prefunctionalised fluorophore (click chemistry,[14] nucleophile substitution,[15] amide coupling,[16] etc.), incorporation of the dye in an inorganic layer coating the magnetic core or incorporation of a fluorescent monomer during the polymerisation step. The latter is one of the most widely used approach; however, it can sometimes be expensive due to price of the fluorescent monomer or even impossible due to the solubility and stability issues associated with the fluorescent monomer, which is often vinyl based. MNs are usually coated with a silica layer to prevent their oxidation and to enable further functionalisation, whereas reducing the number of chemicals and keeping the synthetic procedure as simple as possible are preferred and often required for biomedical applications.

Following the first report on type II photoinitiated precipitation polymerisation for microsphere functionalisation,[17] we recently reported the use of type II photoinitiated polymerisation system to synthesise fluorescent polyacrylamide nanoparticles using Rhodamine B(RhB) and benzophenone (BP), as hydrogen donor and photosensitiser, respectively.[18] The synthesised polymeric nanoparticles are fluorescent, stable and easy to produce, and the size of the nanomaterials could be adjusted by changing monomer concentration. As a continuation of our efforts to find more effective and cost-efficient methods for in situ synthesis and functionalisation of polymers, more recently, we applied this strategy for the synthesis of highly crosslinked and fluorescent polymer microspheres in precipitation polymerisation.[19]

Herein, we aim to expand our previously developed strategy for fluorescent MN synthesis, and investigate the possibility to

Figure 1 Representation of the acrylic acid functionalisation of the nanoparticles, followed by type II-initiated polymerisation of acrylamide and N-N-methylene-bis-acrylamide using the bimolecular system Benzophenone/Rhodamine B. Adsorption configuration is unknown.
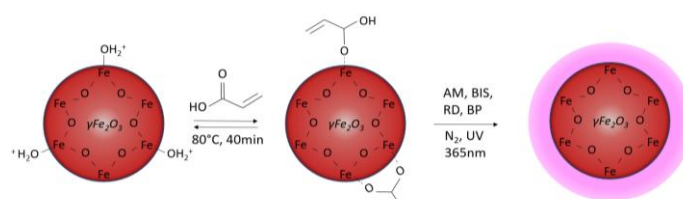
a. *Sorbonne Université, CNRS, Physico-chimie des Électrolytes et Nanosystèmes Interfaciaux, PHENIX, F-75005 Paris, France.*
b. *Saint-Antoine Research Centre (CRSA), INSERM, CNRS, Sorbonne Université, F-75012 Paris, France*
† Footnotes relating to the title and/or authors should appear here.
Electronic Supplementary Information (ESI) available: [Materials, instrumentation, TEM images, DLS, fluorescence microscopy images]. See DOI: 10.1039/x0xx00000x
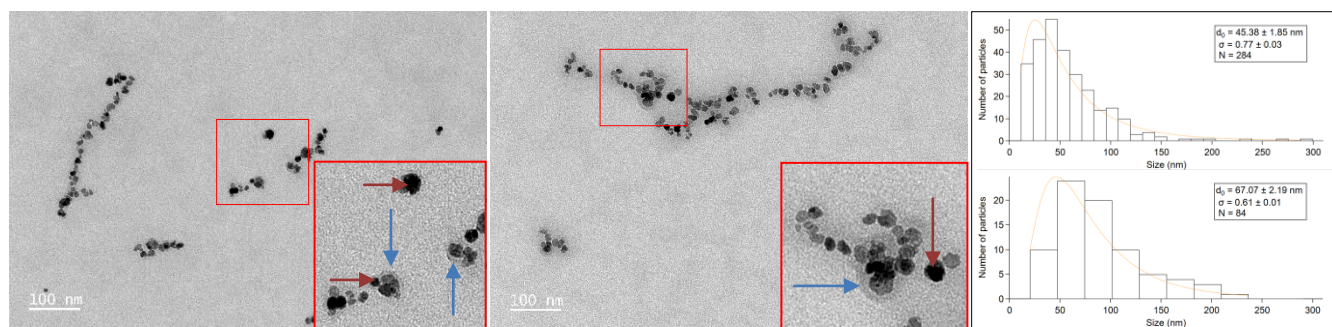
Figure 2 TEM images of samples with an iron to monomer ratio of [1:72] (left) and [1:96] (middle) and the size distribution obtained by analysing those images (right, up and down respectively). The maghemite cores are highlighted by brown arrows and the polymer layer by blue arrows.

use acrylic acid functionalised maghemite nanoparticles to promote in situ polymerisation of a fluorescent polyacrylamide layer through type II photopolymerisation. The synthetic strategy to produce magnetic and fluorescent core-shell NPs is illustrated in Figure 1.

In the first step, maghemite nanoparticles are obtained by coprecipitation of iron (II) and (III), oxidation and sorting of nanoparticles, giving particles in the desired size range (13-16 nm) with good dispersity. Next, MNs were functionalised using acrylic acid through their carboxylic acid moiety, the amount of which was optimised to maximise the incorporated functionality while still maintaining sufficient colloidal stability. After conducting several tests, vinyl functionalised MNs, which satisfy on the abovementioned criteria, were obtained according to the following procedure: 150 µL of acrylic acid (2.175 mmol) was added to 5 mL of MN solution (50.6 mg/mL), which corresponds to 4.535 mmol of iron. The mixture was

[Iron]: [monomer] mole ratio	AaM (mmol)	BIS (mmol)	Size (nm)	Yield (%)	Dry weight (mg)
[1:48]	1.85	0.32	30	74%	134
[1:72]	2.775	0.48	43	19%	51.7
[1:96]	3.7	0.64	95	8.8%	32

then heated to 80°C for 40 min, washed three times with 5 mL of acetone and 5 mL of diethyl ether before being re-suspended in 5 mL of water. Then, MNs were functionalised with a fluorescent polymer shell layer *via* a bimolecular initiation system using RhB and BP as hydrogen donor and photosensitizer, respectively. Upon irradiation at 365 nm, BP is excited to its triplet state and is able to abstract hydrogen from a suitable hydrogen donor to start polymerisation; therefore, the copolymerisation of acrylamide (AaM), N,N-methylenebis(acrylamide) (BIS) and acrylic acid (Aac) adsorbed onto the nanoparticles, is expected to occur through the radical generation on the tertiary amine moiety of the RhB. Table 1 summarises the reaction conditions for core-shell nanoparticles synthesis in this study. Initially, monomer concentration is gradually increased while keeping other

parameters fixed, such as the amount of maghemite nanoparticles (45.3 µmol of iron), BP (22 µmol) and RhB(4.1µmol), as well as AaM to BIS molar ratio ([1:0.17]), irradiation wavelength, time, shaking speed (200rpm) and temperature (25°C).

Table 1 Reaction conditions

Diffusion light scattering measurements reveal that the size of the fluorescent core-shell MNs increases with the monomer concentration (Table 1 and SI). This is not unexpected since the rate of polymerisation is known to increase as the monomer concentration in the reaction mixture is raised. Transmission electron microscopy images of the particles show that the increase in particle size is due to the partial aggregation of MNs, leading to core-shell structures having more nanoparticles inside a thick polymer shell (Figure 2). When the particles synthesised at [1:48] iron to monomer mole ratio, the polymer shell layer is too thin to be observed by TEM (Supplementary Information). Nevertheless, thermogravimetric measurements (Figure 3) and the dry weight of the product after polymerisation (Table 1) reveal that the polymer amount, which are synthesised by using less monomer, is higher in the nanomaterials. This phenomenon can be explained by the fact that the particles prepared by [1:48] iron to monomer ratio contain fewer maghemite nanoparticles, and the total surface area of non-aggregated particles is higher compared with a cluster of aggregated nanoparticles. Hence, even a thinner layer on the particles could result in a higher total amount of polymer. The relatively lower amount of polymer obtained at [1:72] and [1:96] might be attributed to decreasing the initiator to monomer mole ratio.

Nine months after the synthesis, DLS measurements did not show any aggregation of the sample, illustrating its colloidal stability over time (SI).
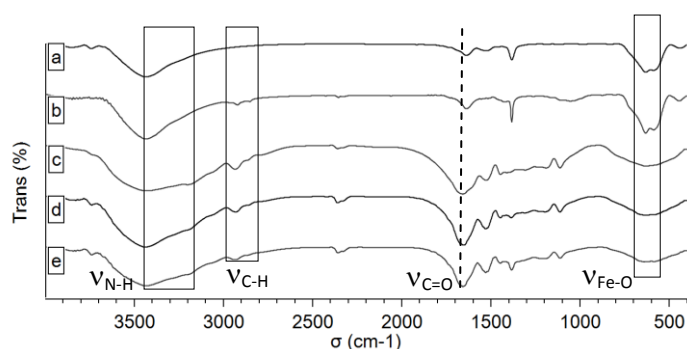
COMMUNICATION

Figure 4 FTIR spectrum of a) naked maghemite nanoparticles, b) Aac functionalised nanoparticles, c) sample [1:48], d) sample [1:72] and e) sample [1:96]

Figure 5 Fluorescence emission spectrum of core-shell samples under an excitation wavelength of 545 nm. [1:48] is 10 time more fluorescent than the others due to its higher polymer content.

The presence of a polymer layer is further supported by Fourier-transform infrared spectroscopy (FTIR) (Figure 4). The successful functionalisation of maghemite nanoparticles by acrylic acid is confirmed by small peaks at 2900 cm^{-1}, corresponding to C-H stretches from AAc (Figure 4.b). All nanocomposites exhibit peaks characteristic for polyacrylamide in their spectra (a broad peak centred at 3400 cm^{-1}, and sharp peaks at 1650 cm^{-1} and 2900 cm^{-1} are assigned for NH_2, C=O, and C-H stretches, respectively) while the maghemite characteristic peaks (628 and 580 cm^{-1} for Fe-O stretches) become harder to distinguish (Figure 4. c-e). The fluorescence spectra of the nanomaterials presented in Figure 5 shows that the material composed of the higher proportion of polymer is also the most fluorescent with an intensity comparable to those previously synthesised using type II photopolymerisation, with a maximum of emission intensity at 585 nm, in accordance with the fluorescent properties of rhodamine B.
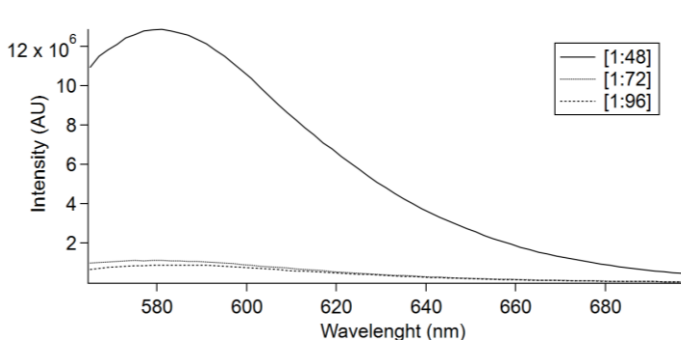
To provide additional evidence of the coupling of magnetic and fluorescent properties of the nanomaterials, a drop of nanomaterial suspension (0.160 mg/mL of iron) was deposited on a microscope slide. As expected, no particle could be observed in bright field with an optical microscope and the fluorescence seems to be homogeneously distributed inside the droplet. Next, a magnet was placed approximately 10 mm away from the sample and the fluorescence at the edge of the droplet was recorded at regular time intervals (15 sec). For all samples, an important increase of fluorescence is observed at the edge of the drop over time, confirming that the nanoparticles are both fluorescent and magnetic. For the sample synthesised with the iron to monomer ratio [1:96] a few small fluorescent aggregates can be observed on the images while the fluorescence on the others remains diffused. Images for sample [1:48] are presented in Figure 6.

Figure 3 TGA analysis of maghemite nanoparticles (NP), acrylic acid functionalised (NP@Aac) and of core-shell samples. While little weight loss is observed for NP and NP@Aac, sample [1:48], [1:72] and [1:96] lose respectively 87%, 79% and 78% of their weight between 200 and 775°C.
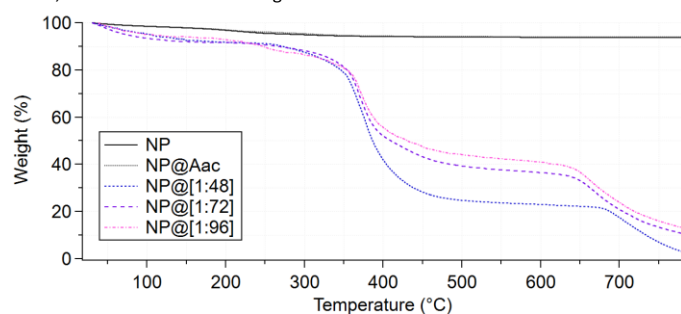
Finally, to compare the developed synthetic strategy with a well-known route, we tested the possibility of synthesising

Figure 6 Fluorescence microscopy images of the edge of a droplet of sample [1:48]. At time 0s, a magnet is deposited on the slide, on the down side, out of the field. Over time, fluorescence is more intense on the edge of the droplet, illustrating both the ability for the magnetic nanoparticles to move under a magnetic field and the coupling between rhodamine B and the magnetic nanoparticles.
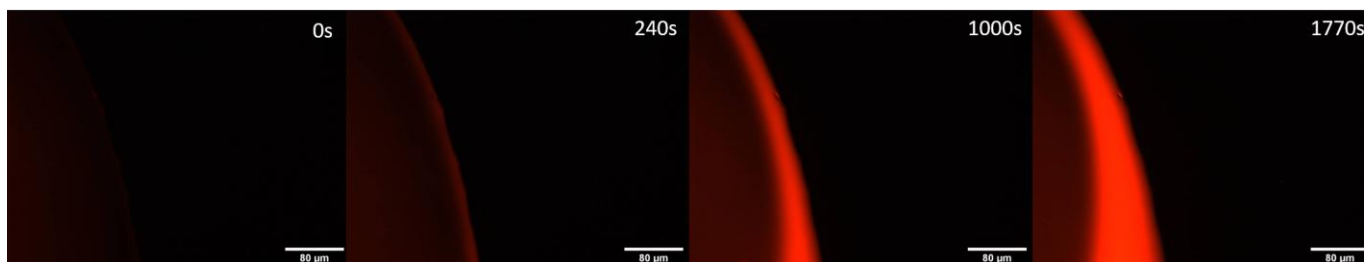
fluorescent core-shell MNs using a fluorescent monomer (acryloxyethylthiocarbamoyl rhodamine B) by redox polymerisation, after surface functionalisation of maghemite nanoparticles using acrylic acid (see SI for details). In absence of fluorescent monomer, similar core-shell structure could be observed on TEM. However, only huge micrometric clusters of magnetic polymers were obtained in presence of the fluorescent monomer, even at very low concentrations.

In conclusion, we developed a new synthetic pathway that allows the synthesis of fluorescent and magnetic core-shell nanoparticles. The size and composition of those nanoparticles make them suitable for biological applications and highly cost effective. The process is versatile and could be applied to several other systems with minor adaptations such as the use of other types of cores (gold, silica, quantum dots…), monomers (thermosensitive, pH degradable…) photosensitiser (to change the wavelength inducing polymerisation). Those modifications could lead to the incorporation of a wide range of new interesting properties. However, the authors are aware that the synthesis can still be improved. In particular, we noted that the synthesis presents an important sensitivity to the temperature and to the mode and speed of shaking, some of those results are presented in SI.

Conflicts of interest

There are no conflicts to declare.

Notes and references

1   P.-W. Lee, S.-H. Hsu, J.-S. Tsai, F.-R. Chen, P.-J. Huang, C.-J. Ke, Z.-X. Liao, C.-W. Hsiao, H.-J. Lin and H.-W. Sung, *Biomaterials*, 2010, **31**, 2425–2434.
2   K. Chatterjee, S. Sarkar, K. J. Rao and S. Paria, *Advances in Colloid and Interface Science*, 2014, **209**, 8–39.
3   P. Mélinon, S. Begin-Colin, J. L. Duvail, F. Gauffre, N. H. Boime, G. Ledoux, J. Plain, P. Reiss, F. Silly and B. Warot-Fonrose, *Physics Reports*, 2014, **543**, 163–197.
4   A. Bossi, S. A. Piletsky, E. V. Piletska, P. G. Righetti and A. P. F. Turner, *Anal. Chem.*, 2001, **73**, 5281–5286.
5   G. Dodi, D. Hritcu, G. Lisa and M. I. Popa, *Chemical Engineering Journal*, 2012, **203**, 130–141.
6   P. Hemström, M. Szumski and K. Irgum, *Anal. Chem.*, 2006, **78**, 7098–7103.
7   W.-C. Wang, K.-G. Neoh and E.-T. Kang, *Macromolecular Rapid Communications*, 2006, **27**, 1665–1669.
8   L. M. de la Rosa-Romo, M. T. Oropeza-Guzmán, A. Olivas-Sarabia and G. Pina-Luis, *Sensors and Actuators B: Chemical*, 2016, **233**, 459–468.
9   K. Mandal, D. Jana, B. K. Ghorai and N. R. Jana, *ACS Appl. Nano Mater.*, 2019, **2**, 3292–3299.
10 S. K. Yen, D. Jańczewski, J. L. Lakshmi, S. B. Dolmanan, S. Tripathy, V. H. B. Ho, V. Vijayaragavan, A. Hariharan, P. Padmanabhan, K. K. Bhakoo, T. Sudhaharan, S. Ahmed, Y. Zhang and S. Tamil Selvan, *ACS Nano*, 2013, **7**, 6796–6805.
11 A. C. Scanone, S. C. Santamarina, D. A. Heredia, E. N. Durantini and A. M. Durantini, *ACS Appl. Bio Mater.*, 2020, **3**, 1061–1070.
12 A. Amani, J. M. Begdelo, H. Yaghoubi and S. Motallebinia, *Journal of Drug Delivery Science and Technology*, 2019, **49**, 534–546.
13 D. Chen, M. Jiang, N. Li, H. Gu, Q. Xu, J. Ge, X. Xia and J. Lu, *Journal of Materials Chemistry*, 2010, **20**, 6422–6429.
14 R. K. O'Reilly, M. J. Joralemon, K. L. Wooley and C. J. Hawker, *Chem. Mater.*, 2005, **17**, 5976–5988.
15 K. Hofmann, I. Kahle, F. Simon and S. Spange, *Beilstein J. Org. Chem.*, 2010, **6**, 0–0.
16 H. Qu, D. Caruntu, H. Liu and C. J. O'Connor, *Langmuir*, 2011, **27**, 2271–2278.
17 T. Bicak, *Macromolecular Chemistry and Physics*, 2021, **222**, 2100022.
18 T. C. Bicak, M. Garnier, M. Sabbah and N. Griffete, *Chem Commun (Camb)*, 2022, **58**, 9614–9617.
19 T. C. Bicak, M. Garnier, M. Sabbah and N. Griffete, *Macromolecular Rapid Communications*, **n/a**, 2200966.